1D Multiscale Modeling of Delignification Rate in Hardwood Chips during Kraft Pulping

I&EC research
Industrial & Engineering Chemistry Research

pubs.acs.org/IECR
Article

1D Multiscale Modeling of Delignification Rate in Hardwood Chips during Kraft Pulping

Carolina Marion de Godoy,[#] Linus Kron,[#] Merima Hasani,[*] and Hans Theliander

Cite This: *Ind. Eng. Chem. Res.* 2026, 65, 12938−12949

ABSTRACT: This paper introduces a multiscale 1D model to describe the delignification inside hardwood chips during kraft pulping. The proposed approach combines our previously developed model encompassing the kinetics of lignin reaction and the transport of lignin fragments inside fiber walls (microscale) with the transport of alkali across the chip (macroscale). Validation was performed using experimental measurements of local lignin content inside birch chips subjected to batch kraft cooking. The results showed it was possible to capture the delignification behavior of the least accessible fibers by focusing on modeling the lignin removal along the thickness of the chip. Additionally, sensitivity analysis indicated the model was heavily influenced by parameters governing the availability of alkali at the chip macroscale. Moreover, similar to what has been reported for softwoods, the model suggests that a virtually uniform delignification could only be achieved under the studied conditions when using thin chips (thickness <2 mm).

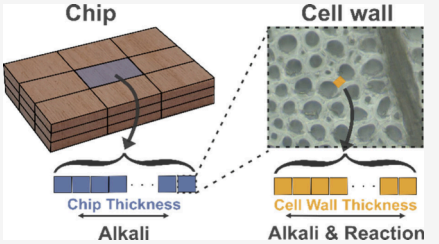

1. INTRODUCTION

The kraft pulping process is central to manufacturing several forest-based products, including many renewable materials that can help reduce society's reliance on fossil carbon. Nevertheless, to meet global demands, it is essential to increase the resource efficiency of the process, including the utilization of finite lignocellulosic feedstocks.[1] Nonuniform delignification should therefore be avoided, as it leads to lower pulping yields, as well as a variance in the properties of the fibers. Thus, effective control of the delignification process during kraft cooking is crucial.[2] However, advancements in this area require a comprehensive understanding of the underlying phenomena taking place during kraft cooking, which involves the simultaneous interplay of various chemical reactions, interphase transport across multiple length scales, and the inherent heterogeneity of the feedstock.[3]

Historically, many modeling efforts describing delignification have emphasized the kinetics of the reactions taking place during kraft cooking, particularly the cleavage of β-O-4 linkages, which was considered the controlling factor in the overall delignification rate.[4] Consequently, numerous mathematical models have focused on these reaction types with varying degrees of complexity.[5] These models frequently assume that the transport of cooking chemicals and dissolved wood components proceeds rapidly, an assumption that faces increasing scrutiny.[6−8] For instance, increased wood chip thickness is known to impact pulping uniformity.[9] Similarly, significant discrepancies have been documented between the chemical environment within the wood chip and the surrounding liquor.[10−12] These observed discrepancies cannot be explained by a strictly reaction-controlled process, indicating that the transport of both chemicals and dissolved wood components is more significant than previously recognized.

In recent years, delignification models have strived to build upon early kinetic models and incorporate the anisotropic nature of wood chips and the different mass transport resistances that impact the process. For instance, Grénman et al.[13] proposed a 3D model in which reaction kinetics was combined with the diffusion of alkali and wood components along the length, width and thickness of chips, accounting for the variations in mass transport resistance caused by changes in porosity and composition of wood during pulping. Gilbert et al.[14] used a different approach: instead of considering the anisotropy of wood, the authors opted for a less complex system, where the wood chips were represented by a solid phase and a liquid phase (entrapped liquor). In this case, the reactions take place in the solid phase, whereas diffusion of wood components and alkali occurs in the entrapped liquor and outside the chip (in the free liquor). A combination of these two strategies was suggested by Bijok et al.[8,15] They proposed adopting the three-phase system mentioned by Gilbert et al. but modeling the diffusion of alkali and wood components in the liquid phases considering the anisotropy of wood, i.e., using distinct effective diffusivities in each direction of the chips.

Received: January 27, 2026
Revised: June 1, 2026
Accepted: June 2, 2026
Published: June 20, 2026

https://doi.org/10.1021/acs.iecr.6c00374
Ind. Eng. Chem. Res. 2026, 65, 12938−12949

These examples, while providing significant advances in modeling kraft cooking, also face criticism. From a phenomenological point of view, the aforementioned models are able to describe the mass transport in the pore system of the chips but lack the explicit description of the transport taking place inside the fiber walls, which has been suggested to limit the delignification rate to some extent.[16,17] In addition, the high computational cost of multidimensional and/or multiscale models can hinder their applicability, limiting their use to operational systems in which memory and CPU time are not restricted, or demanding the development of alternative methods to solve them.[18] Furthermore, model validation often focuses on comparing the predicted results with average data based on lignin content of the pulp throughout cooking. Hence, there is little information regarding how reliable these models are in capturing the lignin gradients inside the chips.

In this context, the present study introduces a simplified multiscale model of delignification in wood chips during batch kraft cooking. The proposed approach expands our previously developed cell wall-level model,[19] combining reaction kinetics, the diffusion of alkali and lignin inside the fiber walls, and the diffusion of alkali across the chip. The goal was to provide a modeling framework that accounts for the main mechanisms limiting the rate of delignification, but with a relatively low complexity, so that the model can be easily adapted and used in industry to predict the defibration point, for example. Thus, the model focuses on describing the delignification of the least accessible fibers, being limited to one dimension (chip thickness) to reduce the computational load. Additionally, the model is validated by comparing simulation results with experimentally determined lignin distributions in wood chips during pulping.

2. MATERIALS AND METHOD

2.1. Model Development

2.1.1. Geometry and General Assumptions. In this multiscale approach, the delignification of a wood chip during kraft pulping was modeled using two characteristic geometries: across the wood chip at the macroscopic level, and within a single fiber wall at the microscopic level, as illustrated in Figure 1. In this geometry, the distance between the lumens of adjacent fibers (i.e., the double wall) was set to 5 μm, which agrees with literature data reported for birch.[20,21] Focused on describing the delignification of the least accessible fibers in the chip, the macroscale of the 1D model was simplified to the radial direction at the center of the chip, i.e., across its thickness (chip thickness = 8 mm). This choice reflects previous findings showing that chip thickness constitutes the critical dimension for diffusion in wood chips,[9,22] as the diffusional path lengths in the longitudinal and tangential directions (i.e., the chip's length and width) are substantially greater, while the effective diffusivities of ions are on the same order of magnitude in all directions under alkaline conditions.[6,23]

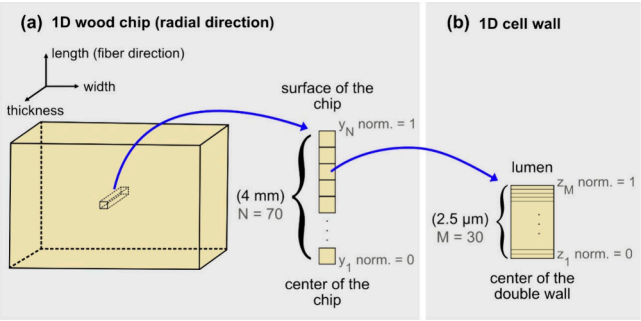

Figure 1. Schematic representation of the geometries considered in the delignification model: (a) radial direction in the middle portion of the wood chip (0.5 × thickness = 4 mm), and (b) a single fiber wall (0.5 × double wall thickness = 2.5 μm). The geometries are based on the hand-cut chips used in the experimental kraft cooking trials. Discretization: wood chip = 70 elements; fiber wall = 30 elements.

To combine the two characteristic geometries, it was assumed that the rate of lignin removal in each element along the radial direction of the chip could be reasonably described by the behavior of a single, representative fiber. Other general assumptions used to develop the model included the following:

a) At the fiber-wall level, the transport of cooking chemicals and the dissolution and transport of lignin followed the framework proposed by Kron et al.[19] In short, Fickian diffusion of lignin fragments limits the delignification in the cell wall, whereas both the diffusion of alkali and the reaction kinetics are comparatively fast.
b) The dissolved lignin fragments and the lignin still bound to the lignocellulosic matrix were described as different species (L_D and L_S, respectively). At the wood chip level, the lignin content (L_C) corresponded to the sum of L_D and L_S still remaining in the fiber wall.
c) Given the uncertainty regarding the influence of hydrosulfide ions on the delignification rate, the current model did not explicitly include a dependency on sulfidity. Instead, the effect of hydrosulfide ions was assumed to be constant. This simplification follows the previous approach applied when modeling the delignification of woodmeal.[19]
d) Carbohydrate reactions were not described explicitly. Instead, the mass of carbohydrates that react at a given time was estimated based on empirical correlations to the mass of lignin in the pulp (refer to Section 2.2).
e) The consumption of hydroxide ions during pulping was approximated by 0.21 g NaOH/g of lignin dissolved and 0.49 g NaOH/g of carbohydrates that reacted (also including neutralization and deacetylation), which are typical values found during kraft pulping of hardwoods.[14,24,25]
f) The transport of dissolved lignin fragments in the wood chip level and their additional reactions with the cooking chemicals were not described explicitly. Still, their impact over the hydroxide concentration should be at least partially accounted for, given the use of experimental correlations for hydroxide consumption. In addition, experimental verification of the degree of delignification was conducted on washed and leached chips, which should reduce the effect any remaining dissolved lignin fragment has on the residual lignin content.
g) The temperature increased with time according to the heating profile used in the pulping experiments (refer to eq 16 in Section 2.3). This temperature rise was quite slow compared to the heat conduction in the wood; therefore, the temperature throughout the chip was assumed to be uniform and equal to the bulk liquor temperature. This assumption is reinforced by the relatively high thermal diffusivity of wood (~3−5 × 10^{-7} m^2/s),[26] resulting in approximately 1 min to achieve a Fourier number of about 1.

2.1.2. Equations: Wood Chip Level. Given the assumptions described in Section 2.1.1, the delignification at the wood chip level was described by the system of PDEs represented in eqs 1 and 2:

$$\frac{\partial L_C}{\partial t} = \frac{\partial \overline{L_S}}{\partial t} + \frac{\partial \overline{L_D}}{\partial t} \tag{1}$$

$$\frac{\partial OH_C}{\partial t} = D_{OH_C}\frac{\partial^2 OH_C}{\partial y^2} - \left(\frac{\partial \overline{OH_W}}{\partial t} - \beta\frac{\partial \overline{L_S}}{\partial t}\right)\left(\frac{1}{\varepsilon} - 1\right) \tag{2}$$

where t is the time, L_C is the lignin content in the wood chip level, which is dependent on the bound (L_S) and dissolved (L_D) lignin in the fiber wall (Section 2.1.3), OH is the concentration of hydroxide

https://doi.org/10.1021/acs.iecr.6c00374
Ind. Eng. Chem. Res. 2026, 65, 12938−12949

ions, denoted by subscript C for the wood chip level and subscript W for the fiber wall level, y is the direction along the thickness of the chip, β is the factor accounting for the consumption of hydroxide ions due to reactions with lignin and carbohydrates (Section 2.2), D_{OH_C} is the effective diffusivity of OH^- along the radial direction of the chip, and ε is the wood chip porosity, which is included to correct for the different volumes occupied by the lignocellulosic matrix and the liquid phase (e.g., the lumens). The overbar notation represents average values across the thickness of the fiber wall.

The effective diffusivity D_{OH_C} was determined based on the diffusivity of sodium hydroxide in water at infinite dilution corrected by the temperature ($D_{OH,free}$) and adjusted according to the local effective capillary cross-sectional area (ECCSA) in the chip. The value of $D_{OH,free}$ was calculated according to Poling et al.,[27] as presented in eqs 3 and 4:

$$D_{NaOH,\infty} = \frac{596.3R}{F^2[(1/\lambda_+) + (1/\lambda_-)]} \tag{3}$$

$$D_{OH,free} = D_{NaOH,\infty}\left(\frac{T}{344\mu_{H2O}}\right) \tag{4}$$

where $D_{NaOH,\infty}$ is the diffusivity of sodium hydroxide in water at 25 °C and infinite dilution, R is the gas constant, F is the Faraday constant, λ_+ is the limiting ionic conductance of Na^+ at 25 °C, λ_- is the limiting ionic conductance of OH^- at 25 °C, T is the temperature of the wood chip, and μ_{H2O} is the viscosity of water at T in centipoise. The calculated values of $D_{OH,free}$ were also used to describe the diffusivity of hydroxide ions in the lumen of the fibers and in the bulk liquor surrounding the wood chip.

To determine D_{OH_C}, the ECCSA of the radial direction of the chip was calculated based on the experimental data from aspen reported by Stone,[23] according to

$$\text{ECCSA} = \begin{cases} 0.4, & OH_C > 0.15 \\ 5.0221OH_C{}^3 - 6.7472OH_C{}^2 + 2.7248OH_C + 0.0969, & 0.0079 \le OH_C \le 0.15 \\ 0.1, & OH_C < 0.0079 \end{cases}$$

$$D_{OH_C} = \text{ECCSA} \times D_{OH,free} \tag{5}$$

in which OH_C is in mol/L.

The initial conditions of eqs 1 and 2 are given by

$$\begin{cases} L_C = 0.94, & t = 0, \forall\, y \\ OH_C = OH_0, & t = 0, \forall\, y \end{cases} \tag{6}$$

The initial L_C value (0.94) is the sum of L_S and L_D at the beginning of pulping (Section 2.1.3), and OH_0 is an estimated initial concentration of hydroxide that was assumed to be uniform throughout the thickness of the chip. Different values of OH_0 were tested, ranging from 0.06 M, which is an average experimental value measured in the center of the wood chip after impregnation, to a limit of 0.55 M (approximately the concentration of hydroxide in the bulk cooking liquor). This range was considered since the consumption factor β already accounts for the total consumption of hydroxide during impregnation, which means OH_0 should represent the alkali content inside the chip after liquor penetration plus the alkali consumed during impregnation due to neutralization and other minor reactions.

The boundary conditions of eq 2 are described by

$$\begin{cases} D_{OH_C}\dfrac{\partial OH_C}{\partial y} = 0, & y = 0 \\ D_{OH_C}\dfrac{\partial OH_C}{\partial y} = D_{OH,free}\dfrac{\partial OH_{Bulk}}{\partial \delta} \cong D_{OH,free}\dfrac{0.55 - OH_C}{5\ \mu\text{m}}, & y = 4\ \text{mm} \end{cases} \tag{7}$$

which correspond to the symmetry of the chip and the mass transfer of hydroxide between the surface of the chip and the surrounding cooking liquor. In this case, the model considered the diffusion of hydroxide ions from the cooking liquor toward the chip, and a linear concentration profile over a layer of 5 μm (approximately the size of the lumen radius) was assumed.

2.1.3. Equations: Cell Wall Level. The delignification at the fiber wall level was modeled following the same procedure described by Kron et al.,[19] resulting in the set of PDEs shown in eqs 8–10:

$$\frac{\partial L_S}{\partial t} = -r_L \tag{8}$$

$$\frac{\partial L_{D,i}}{\partial t} = D_{L_{D,i}}\frac{\partial^2 L_{D,i}}{\partial z^2} + r_L x_i,\ i = [1, 2, ..., 7] \tag{9}$$

$$\frac{\partial OH_W}{\partial t} = D_{OH_W}\frac{\partial^2 OH_W}{\partial z^2} - r_L\beta \tag{10}$$

where r_L is the effective reaction rate (representing all reactions which contribute toward solubilizing lignin from the lignocellulosic matrix), $L_{D,i}$ is the ith size fraction of the dissolved lignin remaining in the fiber wall, $D_{L_{D,i}}$ is the effective diffusivity of the corresponding lignin fraction, x_i is the mass fraction of the ith lignin fraction, OH_W is the hydroxide concentration in the cell wall, and z is the spatial direction along the fiber wall thickness. More details regarding the motivation and application of the dissolved lignin fractions can be found in the previous paper.[19] In the original model, the diffusivity of hydroxide in the cell wall (D_{OH_W}) was assigned a single constant value. The current work extended this to include a temperature dependence based on the expression developed by McKibbins,[28] with the same activation energy. The pre-exponential factor was scaled to correspond to 10^{-11} m^2/s at room temperature, which was the value previously used.[19] It is possible the diffusivity could be closer to an order of magnitude larger, as indicated in studies focused on ozone bleaching,[29] although it is difficult to compare such systems with kraft pulping, since the flexibility and swelling of the fibers may differ substantially due to the distinct process conditions (e.g., pH) and degrees of delignification. However, as shown in our original cell wall model, the effect of alkali transport within the cell wall is negligible even using the present conservative diffusivity value. The resulting expression of D_{OH_W} is presented in eq 11:

$$D_{OH_W} = 2.5 \times 10^{-9}\sqrt{(T)}\, e^{-\frac{4870}{RT}} \tag{11}$$

where T is the temperature in kelvin, and R is the thermodynamic gas constant in cal/(mol K).

The initial conditions assumed a reduced starting concentration of the bound lignin to account for the easily soluble fraction of lignin which is removed even at room temperature. This value was estimated from measurements of the Klason lignin content in the center of the chip 15 min into the process, before the target cooking temperature had been reached.[30] The initial concentration of dissolved lignin was assumed zero, and the OH^- level was assumed identical in the fiber wall as in the chip. The boundary conditions were defined on similar premises as in the model by Kron et al., with the exception that the hydroxide gradient across the lumen was now evaluated using the local concentration in the chip, OH_C, rather than the bulk concentration in the surrounding liquor. The following initial and boundary conditions are presented in eqs 12 and 13:

$$\begin{cases} L_S = 0.94, & t = 0, \forall\, z \\ L_D = 0, & t = 0, \forall\, z \\ OH_W = OH_0, & t = 0, \forall\, z \end{cases} \tag{12}$$

https://doi.org/10.1021/acs.iecr.6c00374
Ind. Eng. Chem. Res. 2026, 65, 12938−12949

$$\begin{cases} \dfrac{\partial OH_W}{\partial z} = \dfrac{\partial L_S}{\partial z} = \dfrac{\partial L_D}{\partial z} = 0, & z = 0 \\ D_{L_{D,i}} \dfrac{\partial L_{D,i}}{\partial z} = D_{L_B} \dfrac{\partial L_{D_B}}{\partial \delta} \cong D_{L_B}\left(-\dfrac{L_{D,i}}{5\ \mu m}\right), & z = 2.5\ \mu m \\ D_{OH_W} \dfrac{\partial OH_W}{\partial z} = D_{OH,free} \dfrac{\partial OH_B}{\partial \delta} \cong D_{OH,free} \dfrac{OH_C - OH_W}{5\ \mu m}, & z = 2.5\ \mu m \end{cases} \quad (13)$$

where the gradient of dissolved lignin in the lumen $\left(\frac{\partial L_{D_B}}{\partial \delta}\right)$ was assumed to be linear, decreasing from $L_{D,i}$ at the cell wall surface to zero at the center of the lumen (5 μm, which is approximately the radius of the lumen). Similar assumptions were applied to $\frac{\partial OH_B}{\partial \delta}$, although in this case, the lumen concentration corresponded to the simulated concentration in the wood chip node, OH_C, instead of zero. The subscript B denotes conditions in the lumen.

2.2. Parameter Analysis and Model Evaluation

In the model, a consumption factor (β) was used to describe the consumption of hydroxide ions in reactions with lignin and carbohydrates. This factor was calculated according to eq 14:

$$\beta = \frac{(0.21 + 0.49\alpha)\rho_L L_0}{M_{NaOH}} \quad (14)$$

where 0.21 and 0.49 are, respectively, the consumptions of sodium hydroxide per mass of lignin and per mass of carbohydrates that reacted during pulping (as mentioned in Section 2.1.1). ρ_L is the density of wood substance, which was approximated by 1500 kg/m^3. M_{NaOH} is the molar mass of sodium hydroxide and L_0 is the content of lignin in the wood before pulping, which was measured (L_0 = 0.193 g Klason lignin/g odw). Since carbohydrates are not represented explicitly in the model, the mass of carbohydrates that reacted at a given time was estimated based on the amount of lignin reacted. In eq 14 this is represented by α, that is the ratio between carbohydrates and lignin that remain in the pulp after a given time of cooking. This ratio was determined experimentally for the chips used in this study, as shown in Figure 2.

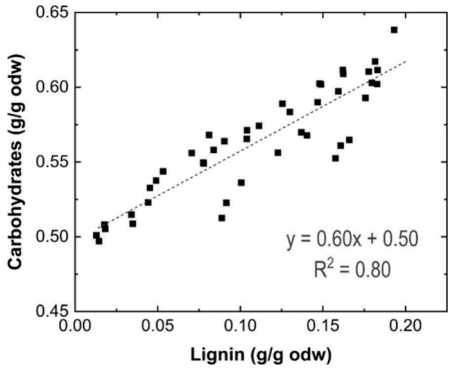

Figure 2. Carbohydrates remaining in the pulp (g/g odw) as a function of Klason lignin in the pulp (g/g odw). Data from the experiments of Marion de Godoy et al.[30]

As the data from Figure 2 do not extend into the final stage of delignification, which is known to have a greater extent of carbohydrate removal relative to lignin, a second carbohydrate/lignin-ratio was fitted to the data of Kron et al.[19] The resulting expression for α is given in eq 15.

$$\begin{cases} \alpha = 0.60, & 0.010 \le \text{lignin} \le 0.193 \\ \alpha = 7, & \text{lignin} < 0.010 \end{cases} \quad (15)$$

2.3. Experimental Data

The experimental data used to evaluate the model was acquired in earlier studies.[30,31]

Batch kraft cooking experiments were conducted using hand-cut chips of birch, as described in previous work.[30] Initially, the chips were placed in autoclave vessels together with white liquor. They were impregnated (partial vacuum using a water aspirator for 10 min, followed by pressurization with 5 bar N_2/ 20 min) after which the vessels were placed in a preheated polyethylene glycol bath under agitation. The temperature profile inside the vessels followed the equation derived by Bogren et al.[32]

$$T = T_B - (T_B - 293.15)e^{-t/(918 - 1.26T_B)} \quad (16)$$

where T is the temperature inside the vessel, and T_B is the temperature of the cooking bath (both in K).

Table 1 summarizes the experimental conditions utilized during cooking:

Table 1. Cooking Conditions and Liquor Composition

Parameter	Value
T_B (K)	438.15
Time (min)	15, 30, 45, 60
[OH^-] (mol/kg liquor)	0.55
[SH^-] (mol/kg liquor)	0.25
Na_2CO_3 (mol/kg liquor)	0.10
Liquor:wood (w:w)	22:1

After reaching the desired cooking time, the process was stopped by placing the vessels in a cooling bath. The chips were separated from the black liquor via vacuum filtration and washed with 2 L of distilled water. To remove any residual liquor, the chips were leached in distilled water for about 2 weeks (leaching water was changed every other day).

To assess the composition in the middle of the chips, they were cut to separate sides, corners, and the center. Next, the center piece was sliced into different layers (surface, intermediate and inner layer) with 1−1.5 mm each. Each layer was subjected to acidic hydrolysis to determine the Klason lignin content, providing the lignin gradient used to evaluate the goodness of fit of the model.

To measure the average hydroxide content in the middle portion of the chip at the beginning of cooking, wood chips were collected right after impregnation and placed in liquid nitrogen for 5 min. These samples were then cut into different pieces and placed in distilled water. They were left leaching in water at room temperature overnight, under constant agitation. The following day the hydroxide content was determined by titrating the leaching water with HCl (end point = pH 7). More details about the determination of hydroxide content are mentioned elsewhere.[30]

3. RESULTS AND DISCUSSION

3.1. Model Response: Original Parameters

3.1.1. Radial Profile. Figure 3 shows radial lignin gradients in the chips at different pulping times according to experimental data and model predictions when setting OH_0 to 0.06 and 0.55 M. The corresponding simulated profiles of lignin content and hydroxide concentration across the thickness of the chip over time are displayed in Figure 4. All the lignin data presented in the Results and Discussion section have been normalized to the initial content of lignin in the untreated wood (0.1930 g/g odw), as measured in previous work.[30]

When comparing the modeled lignin gradients in Figure 3, it is apparent that the starting concentration of hydroxide (OH_0) had a considerable impact on the simulated extent of

https://doi.org/10.1021/acs.iecr.6c00374
Ind. Eng. Chem. Res. 2026, 65, 12938−12949

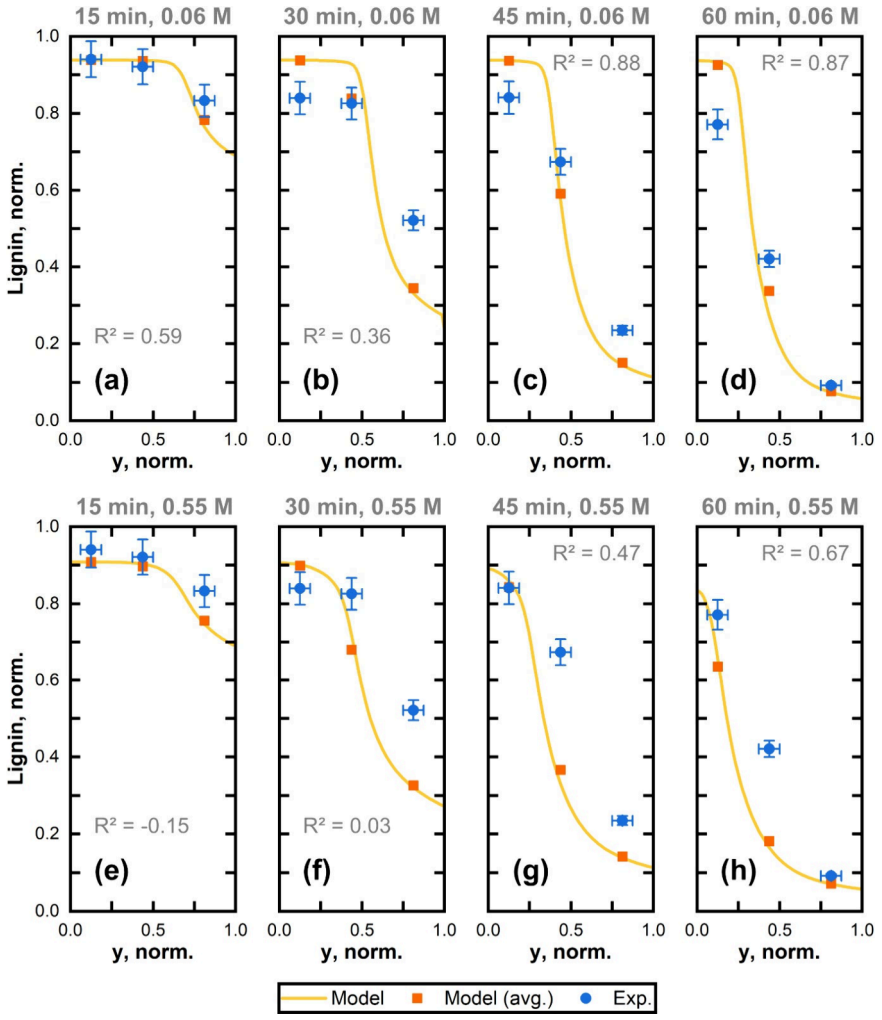

Figure 3. Normalized Klason lignin content over the radial direction in the middle of the wood chip (refer to Figure 1). First line: results achieved after (a) 15 min, (b) 30 min, (c) 45 min, and (d) 60 min of cooking when using OH_0 = 0.06 M. Second line: results achieved after (e) 15 min, (f) 30 min, (g) 45 min, and (h) 60 min of cooking when using OH_0 = 0.55 M.

delignification across the thickness of the chip. Interestingly, this impact increased with pulping time, being more pronounced after 45 and 60 min compared to 15 and 30 min. In both scenarios, OH^- was virtually depleted in the center of the wood chip within 10 min, as indicated in Figures 4b and 4d. If the initial OH^- concentration had influenced only the early extent of delignification—simply causing more lignin to react before the depletion of alkali in the 0.55 M case—then any difference between the two scenarios would have remained unchanged after this point. However, this was not observed, implying that the initial OH^- concentration has a relatively long-lasting influence on the overall delignification rate. A likely explanation is the increased influx of alkali occurring when using a high OH_0 value, which is driven by the higher swelling of wood (represented by the increasing ECCSA in the model, see eq 5). This effect is visible in Figure 4, where the OH^- gradient penetrates further into the chip for the 0.55 M case compared with the 0.06 M case.

The results in Figure 4 also show that, regardless of OH_0, lignin and hydroxide displayed essentially inverse profiles. This suggests that the hydroxide ions were not readily available within the wood; otherwise, the delignification would have progressed more uniformly across the chip. Furthermore, after significant delignification near the surface, a steep lignin gradient developed and gradually moved inward over time, although the chip center remained largely undelignified even after 60 min. Meanwhile, the predicted OH^- gradient was approximately linear and penetrated progressively deeper into the chip, indicating that hydroxide diffusion was slow relative to its consumption.

3.1.2. Longitudinal Profile. To verify the soundness of modeling the delignification of the chip center using a 1D approach across the chip thickness, the proposed model was also used to describe the lignin removal along the longitudinal direction of the chip (Figure 5a). For this simulation, the ECCSA was set to 0.51, regardless of the local concentration of alkali, following the data reported by Stone.[23] In addition, the chip half-length in the longitudinal direction was set to 1.5 cm, i.e., 3.75 times longer than in the radial case, and the initial hydroxide concentration (OH_0) was 0.55 M. Figure 5b shows the predictions of the model for the longitudinal lignin gradients in the chips at different pulping times compared to experimental data.

Based on Figure 5b, it is evident that the extent of lignin removal observed in the chip center was not captured by modeling the longitudinal transport of alkali alone. This behavior reflects the increase in the characteristic time for the diffusion of OH^-, defined by $\tau = l^2/D_{OH^-}$, which, depending on

https://doi.org/10.1021/acs.iecr.6c00374
Ind. Eng. Chem. Res. 2026, 65, 12938−12949

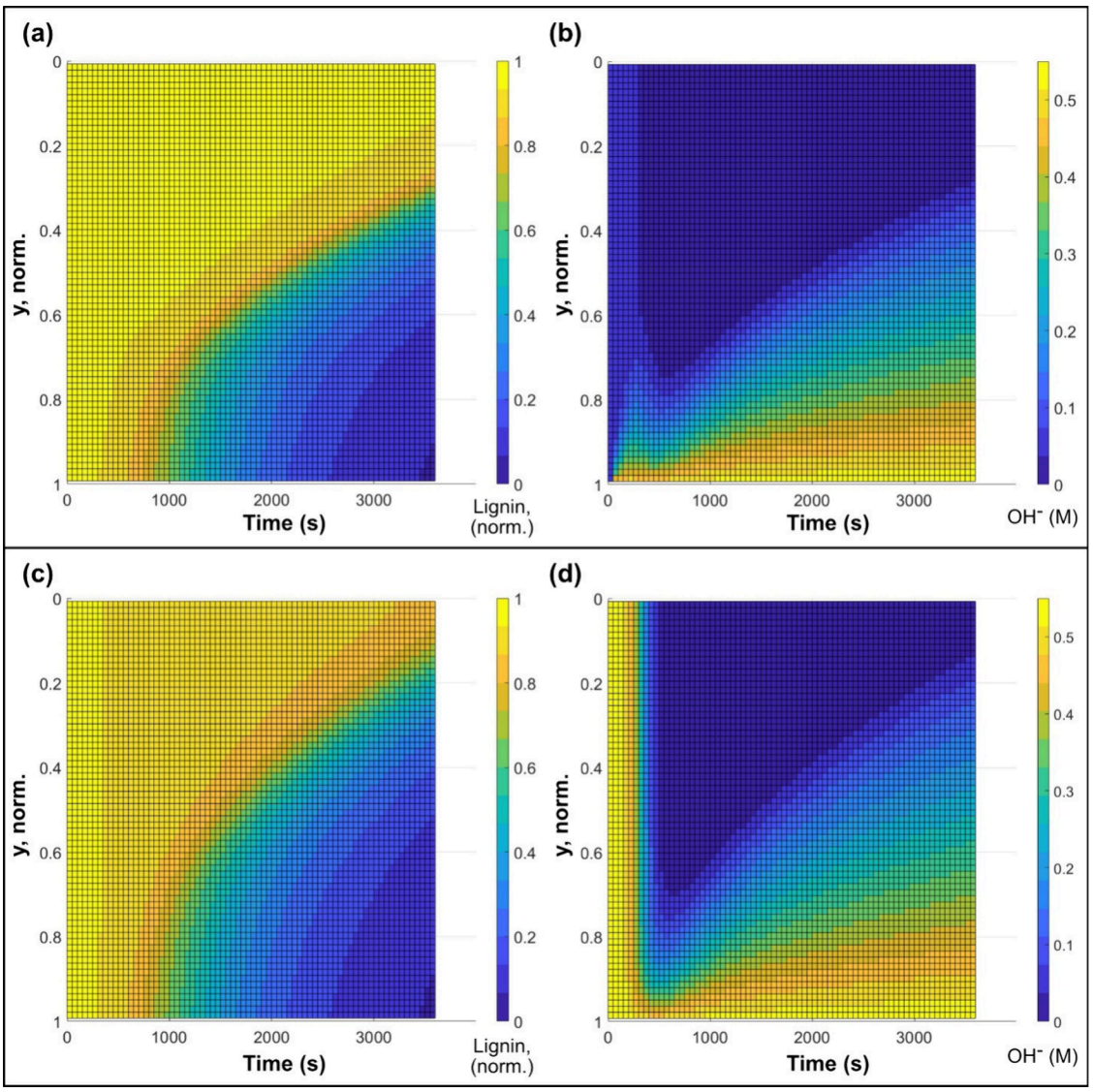

Figure 4. Concentration profiles across the radial direction of the wood chip over time. Distribution of (a) Klason lignin and (b) hydroxide ions, as predicted by the model with OH_0 = 0.06 M. Distribution of (c) Klason lignin and (d) hydroxide ions, as predicted by the model with OH_0 = 0.55 M.

the local concentration of alkali, was roughly 3−11 times higher in the longitudinal case than in the radial case. Consequently, the delignification predicted by the model in the central portion of the chip had no substantial contribution from the longitudinal transport of alkali. This reinforces the importance of the radial transport of alkali as the major driver of delignification in the least accessible fibers. Furthermore, similar conclusions can be drawn from the predicted distributions of lignin and hydroxide content along the length of the chip (Figure 6), as they indicate the complete depletion of alkali (concentration $<10^{-4}$ M) at a distance of 6 mm from the chip surface.

3.1.3. Sources of Model Uncertainties. Regarding the goodness of fit of the model, Figure 3 indicates two main discrepancies between predicted and experimental data. First, the model with the original parameters consistently overestimated the degree of delignification at the point closest to the surface (y ≈ 0.8) for the intermediate (30 and 45 min) time points. Second, the model underestimated the degree of delignification at the center of the chip toward the longer times (i.e., 45 and 60 min, position y ≈ 0.1). These shortcomings probably arise due to inaccuracies in the value of some parameters and due to specific assumptions made when developing the model.

One example of uncertainty is related to the original hydroxide content (represented by parameter OH_0), which most likely varies according to the position in the chip (y) and can assume values between 0 and 0.55 M. Another parameter with a high degree of uncertainty is the effective diffusivity of hydroxide ($D_{OH,r}$). To calculate the values of $D_{OH,r}$, the local ECCSA values inside the chip were estimated based on literature data, which was collected after exposing a different hardwood species (aspen) to alkaline media for several hours at room temperature. Hence, the current values used in the model may not reflect the real effective diffusivity of hydroxide in birch wood under pulping conditions. In fact, the values may overestimate the actual effective diffusivity of hydroxide, partly due to the relatively short pulping time used in this study and partly because the experiments were conducted on a denser wood species (birch) than the original aspen data.

https://doi.org/10.1021/acs.iecr.6c00374
Ind. Eng. Chem. Res. 2026, 65, 12938−12949

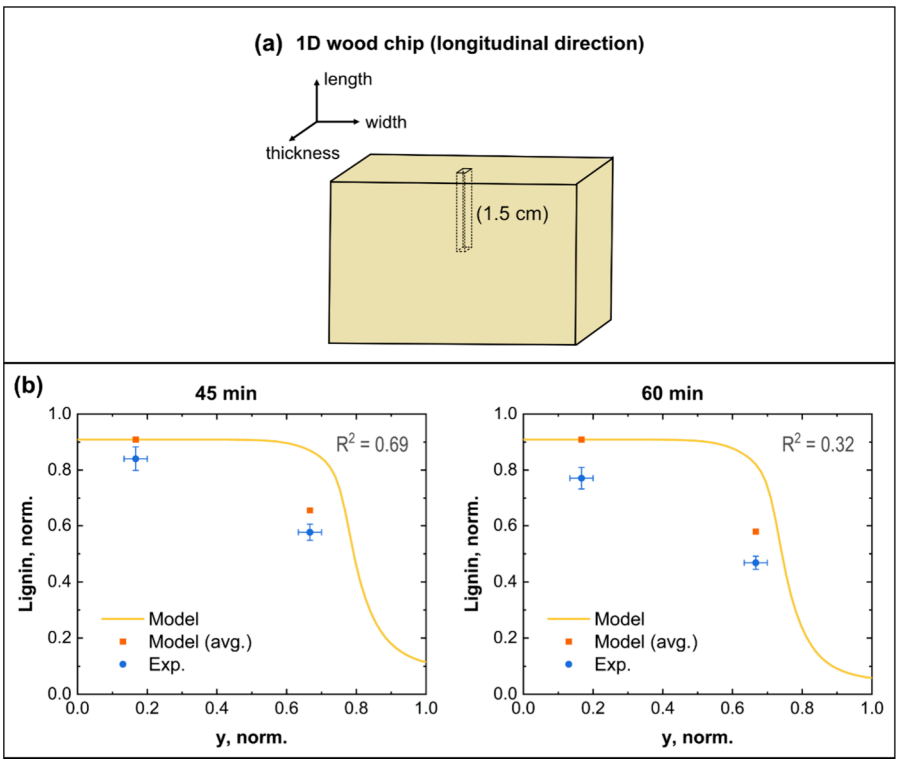

Figure 5. Delignification across the longitudinal direction of the chip: (a) scheme illustrating the new geometry of the model; (b) normalized lignin content in the middle of the wood chip across the longitudinal direction at 45 min of cooking (on the left) and 60 min of cooking (on the right). Model parameters: ECCSA = 0.51, OH_0 = 0.55 M.

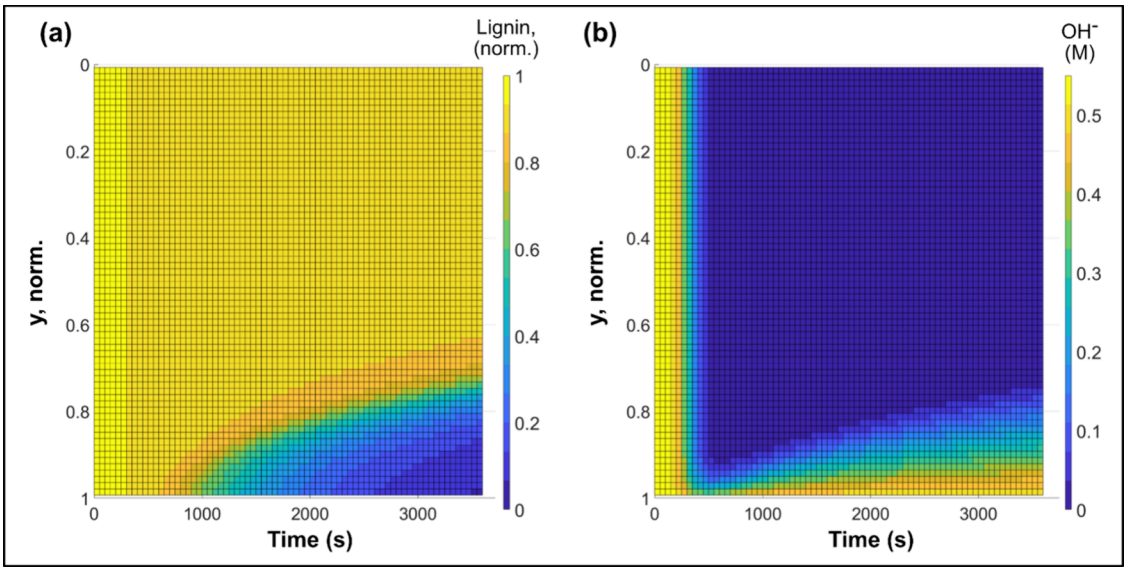

Figure 6. Distribution of (a) Klason lignin and (b) hydroxide ions across the longitudinal direction of the wood chip over time. Model parameters: ECCSA = 0.51, OH_0 = 0.55 M.

In terms of assumptions, hydroxide ion consumption in lignin- and carbohydrates-related reactions (used to calculate β) was simplified to a single parameter for each component: 0.21 g NaOH/g and 0.49 g NaOH/g, respectively. Although this simplification is common practice,[14,24,25] it fails to capture the complex interplay of the various alkali-consuming reactions. In particular, the consumption factors were assumed to be constant, despite the fact that most of the alkali consumption associated with carbohydrates occurs at the beginning of pulping. For example, reactions mainly targeting hemicelluloses (e.g., deacetylation and peeling) account for the majority of the alkali consumption[3,33] and predominantly occur early in the process,[34,35] yet no distinction was made between them and cellulose-related reactions in this framework.

Another relevant simplification relates to assuming a constant effect of sulfidity on the delignification rate. As discussed in connection with Figure 4, OH^- diffusion was relatively slow, suggesting that HS^- transport may have been similarly constrained. However, alkali availability is also

https://doi.org/10.1021/acs.iecr.6c00374
Ind. Eng. Chem. Res. 2026, 65, 12938−12949

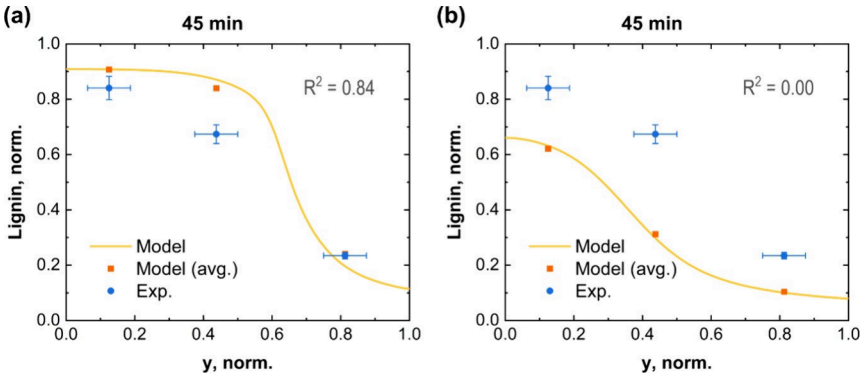

Figure 7. Normalized Klason lignin content over the radial direction in the middle of the wood chip after 45 min of cooking, using (a) the reduced ECCSA or (b) the reduced intrinsic reaction rate. In both cases the initial OH^- was 0.55 M.

influenced by its consumption in various reactions. Although OH^- consumption far exceeds that of HS^-, sulfidity levels do vary during delignification.[36,37] It is therefore reasonable to expect a limited availability of HS^- in the chip center, albeit to a lesser extent than OH^-. Consequently, the simplification of constant HS^- concentration should lead to an overestimation of delignification at the chip center, but this effect was not observed in the simulated data. An additional issue regarding the assumption of constant HS^- concentration concerns modeling systems that operate with different sulfidity levels than those applied to estimate the kinetic parameters of the model. In fact, the kinetic parameters at the cell wall scale were adjusted based on pulping data acquired using 0.15 M HS^-/kg liquor,[19] which represents a lower sulfidity than that applied during the experiments used in this study. However, as the kinetic role of HS^- is not yet fully understood, further research is required to overcome these limitations and explicitly account for sulfidity in the model.

3.2. Sensitivity Analysis

During the development of the model, the value of OH_0 was further varied in the range of 0.06−0.55 M. Simultaneously, the carbohydrate/lignin ratio α was varied based on the experimental results of our previous work.[12] A discussion detailing the analysis of the model based on these variables is included in the Supporting Information. Regardless, these attempts only achieved a somewhat improved fit. Moreover, the issues highlighted in Section 3.1.3 remained, i.e., lignin removal was overestimated by the model at the surface of the chip and it was underestimated at the center, where the results predicted the depletion of alkali. Hence, the analysis of the model was then focused on parameters directly affecting the profile of alkali in the chip, including the effective diffusivity of hydroxide and the kinetics of alkali consumption.

To address the first discrepancy, the value of ECCSA was decreased, which should mainly affect the rate of alkali diffusion at the surface of the chip, where the total OH^- concentration is high. As an initial test, the ECCSA was set to 0.1 (i.e., that of unswollen wood), regardless of OH^- concentration. While this change represents an extreme scenario, the results in Figure 7a demonstrate that it is possible to capture the slower delignification at the surface of the chip by decreasing the ECCSA, as evidenced by the comparison with Figure 3g. As previously discussed, this adjustment may also more closely reflect the actual conditions associated with shorter pulping times, since the swelling of wood is not instantaneous.[6] In addition, a small ECCSA could be more appropriate to describe denser wood species such as birch.

Second, the lignin reaction rate was altered. In the model by Kron et al.,[19] the simulated reaction rate corresponded to a complete conversion of the bound lignin, L_S, in about 5 min (at 150 °C). As noted in the original study, although this represented the best fit to the experimental data, the actual reactions solubilizing lignin likely persist for longer times, albeit still shorter than what has traditionally been considered. For example, it has previously been suggested that the lignin cleavage reactions may be as fast as 10−20 min.[38] Moreover, our recent data suggests that rate-affecting reactions, likely related to demethylation, are significantly diminished after about 60 min.[39] Therefore, the parameter optimization of the original model was performed again, with constraints on the reaction rate. An acceptable fit was found, corresponding to a reaction rate about 4 times slower (more details available in the Supporting Information). However, since this new cell wall model was still fitted to the same original data, the *apparent* reaction rate, i.e., the combined effect of reaction and diffusion in the cell wall, remained essentially the same.

The results of the updated model are displayed in Figure 7b. As apparent from comparison with Figure 3g, the modified reaction parameters had a rather large impact on the overall delignification, despite the unchanged apparent delignification rate. A probable reason is that the slower intrinsic reaction rate results in a slower consumption of alkali, which allows more OH^- to penetrate further into the wood chip. In the first case (i.e., fast reaction) the OH^- was completely depleted at the center of the wood chip, reaching simulated values of $\sim 10^{-10}$ M. In contrast, when the reaction rate was reduced, the level of OH^- never dropped below 10^{-4} M. This difference in available OH^- appears to be enough for, albeit slow, reaction and diffusion of the dissolved lignin fragments to occur even in the center, resulting in the more homogeneous profile of Figure 7b. Additionally, it is worth mentioning that the longitudinal transport of alkali remained negligible at the chip center after reducing the intrinsic reaction rate, as shown in the Supporting Information.

3.3. Model Response: Adjusted Parameters

The synergistic effects of reducing the intrinsic reaction rate and decreasing the ECCSA were combined through manual iterative adjustment, resulting in a constant ECCSA value of 0.20 (regardless of hydroxide concentration), an OH_0 equal to 0.31 M, and the slower intrinsic reaction rate discussed in Section 3.2. A summary of the parameters used in the model is

https://doi.org/10.1021/acs.iecr.6c00374
Ind. Eng. Chem. Res. 2026, 65, 12938−12949

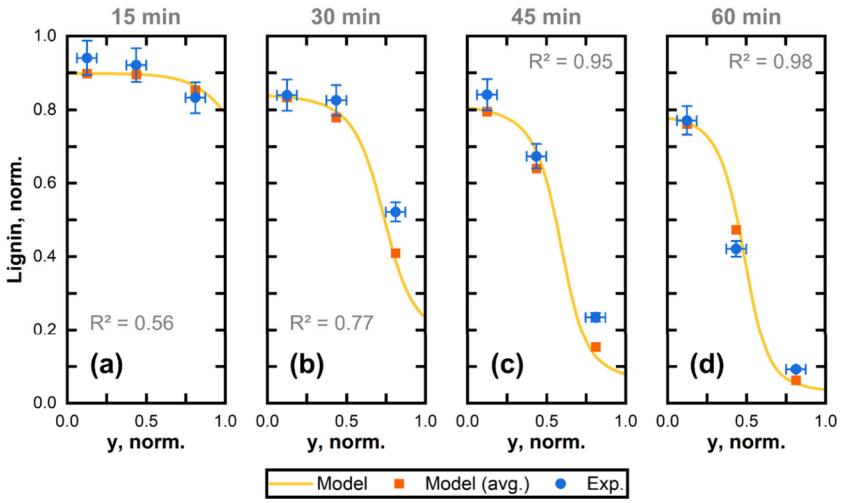

Figure 8. Normalized Klason lignin content over the radial direction in the middle of the wood chip for (a) 15 min, (b) 30 min, (c) 45 min, and (d) 60 min of cooking. Model parameters: low intrinsic reaction rate (~20 min) and low effective diffusivity (ECCSA = 0.20). Initial alkali concentration = 0.31 M.

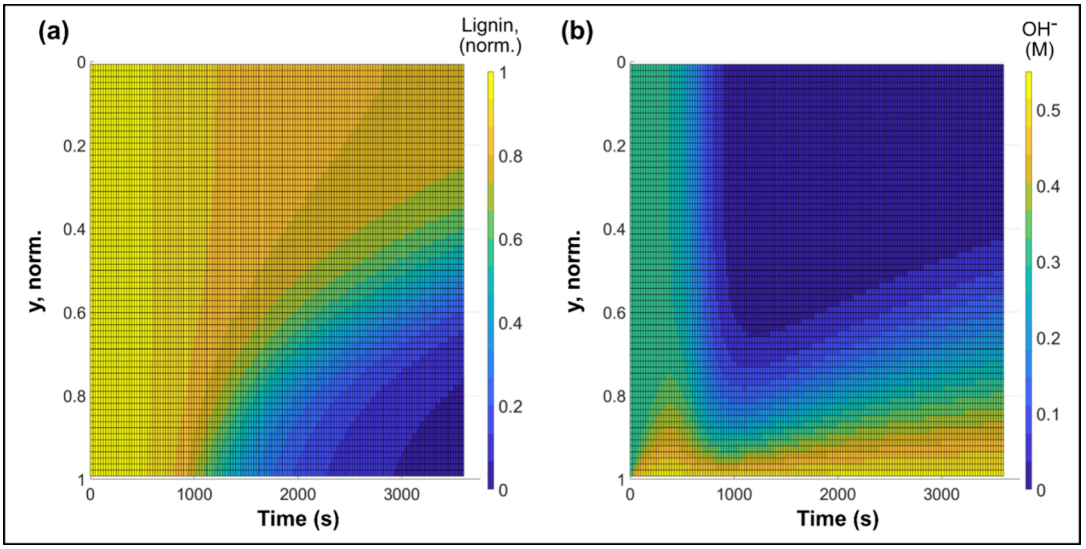

Figure 9. Distribution of (a) Klason lignin and (b) hydroxide ions across the radial direction of the wood chip over time. Model parameters: low intrinsic reaction rate (~20 min) and low effective diffusivity (ECCSA = 0.20). Initial alkali concentration = 0.31 M.

provided in the Supporting Information. As illustrated in Figure 8, the new parameters allowed the model to capture the radial gradient of lignin in the chip throughout the whole experiment. However, it is worth noting that the purpose of the altered parameters is not to represent the best fit to the experimental data, nor provide accurate estimates of physical data. Instead, these results demonstrate the model's capability to capture the physical trends of the experimental data, while simultaneously highlighting its sensitivity to the altered parameters.

Figure 9 shows the modeling results in terms of lignin and alkali distribution within the wood chip over time when utilizing the new parameters. By comparing the profiles in Figures 9a,b, it is clear that the availability of OH^- continued to be a limiting factor to the progression of delignification inside the chip, as suggested by the uneven removal of lignin. However, unlike the results shown in Figure 4, the center of the wood chip never reached a complete depletion of alkali. Instead, delignification occurred throughout the whole thickness of the chip, but the rate varied according to the local hydroxide concentration.

From a more practical point of view, the profiles in Figure 9 also suggest that a nearly homogeneous delignification could be achieved under these pulping conditions if a chip with up to 30% of the current thickness was used (i.e., a chip with about 2−3 mm of thickness). This result agrees with the data reported by Gullichsen et al.,[40] although their experiments focused on lignin removal in softwood chips.

4. CONCLUSION

A multiscale model describing the delignification of wood chips during kraft pulping was developed by coupling diffusion-dependent delignification within fiber walls with the transport of hydroxide ions across one dimension of the chip. The results highlighted the following:

- The model was able to capture the progression of delignification inside wood chips. Accordingly, one-dimensional modeling across the chip thickness was

https://doi.org/10.1021/acs.iecr.6c00374
Ind. Eng. Chem. Res. 2026, 65, 12938−12949

sufficient to represent delignification in the chip core, as longitudinal transport effects were comparatively minor.

- The agreement with the experimental data was further improved by adjusting the effective diffusivity of hydroxide ions and the intrinsic reaction rate. These adjustments highlight the model's sensitivity to alkali availability at the chip scale, indicating that mass transport limitations at this level significantly influence the overall delignification rate throughout the process.
- A more accurate description of the delignification profiles may require improved modeling of alkali consumption and explicit incorporation of sulfidity effects.
- The results further indicate that chip thickness plays an important role in the uniformity of lignin removal. Consequently, an increasingly uneven delignification is expected in chips with thicknesses greater than 2−3 mm.

■ ASSOCIATED CONTENT

Data Availability Statement

The data files are available upon reasonable request from the corresponding author.

Supporting Information

The Supporting Information is available free of charge at https://pubs.acs.org/doi/10.1021/acs.iecr.6c00374.

Detailed sensitivity analysis of model parameters (initial concentration of hydroxide and ratio between unreacted carbohydrates and lignin); description of parameter re-estimation; model response in the longitudinal direction using re-estimated parameters; derivation of eq 2; and model parameters (PDF)

■ AUTHOR INFORMATION

Corresponding Author

Merima Hasani − *Department of Chemistry and Chemical Engineering and Wallenberg Wood Science Center, Chalmers University of Technology, SE-412 96 Gothenburg, Sweden*; Email: merima.hasani@chalmers.se

Authors

Carolina Marion de Godoy − *Department of Chemistry and Chemical Engineering, Chalmers University of Technology, SE-412 96 Gothenburg, Sweden*

Linus Kron − *Department of Chemistry and Chemical Engineering, Chalmers University of Technology, SE-412 96 Gothenburg, Sweden*; orcid.org/0000-0003-3510-9826

Hans Theliander − *Department of Chemistry and Chemical Engineering and Wallenberg Wood Science Center, Chalmers University of Technology, SE-412 96 Gothenburg, Sweden*; orcid.org/0000-0002-2120-6513

Complete contact information is available at: https://pubs.acs.org/10.1021/acs.iecr.6c00374

Author Contributions

#C.M.d.G. and L.K. share first authorship. All authors contributed to the study conception and design. Modeling and data analysis were performed by C.M.d.G. and L.K. All authors contributed to the interpretation of the results. The first draft of the manuscript was written by C.M.d.G. and L.K. All authors commented on previous versions of the manuscript. All authors read and approved the final manuscript.

Funding

This work was performed within the strategical innovation program BioInnovation - a joint initiative by Vinnova (Sweden's innovation agency), Formas (a Swedish research council for sustainable development), and the Swedish Energy Agency.

Notes

The authors declare no competing financial interest.

■ ACKNOWLEDGMENTS

The collaboration and financial support of the Resource-smart Processes Network, financed by Vinnova via BioInnovation and industrial partners (Billerud, Holmen, SCA, Stora Enso, Södra Skogsägarna, and Valmet), is gratefully acknowledged.

■ ABBREVIATIONS

ECCSA Effective capillary cross-sectional area, [-]

Symbols

F	Faraday constant, [C/g_{equiv}]
$D_{L_{D,i}}$	Diffusivity of dissolved lignin (reacted lignin) in the cell wall, fraction i = [1, 2, ..., 7], [m^2/s]
$D_{NaOH,\infty}$	Diffusivity of NaOH in water at 298 K, [m^2/s]
D_{OH}	Effective diffusivity of alkali, [m^2/s]
$D_{OH,free}$	Diffusivity of NaOH in water at infinite dilution corrected by temperature, [m^2/s]
L_0	Mass fraction of Klason lignin in the wood before pulping, [-]
L_C	Relative mass concentration of lignin in the wood chip, [-]
L_D	Relative mass concentration of all dissolved (reacted) lignin fractions in the cell wall, [-]
$L_{D,i}$	Relative mass concentration of dissolved (reacted) lignin in the cell wall, fraction i = [1, 2, ..., 7], [-]
L_S	Relative mass concentration of solid/unreacted lignin in the cell wall, [-]
l	Characteristic length of diffusion, [m]
M	Number of discretized elements at the cell wall scale, [-]
M_{NaOH}	Molar mass of NaOH, [mol/m^3]
N	Number of discretized elements at the wood chip scale, [-]
OH_0	Initial concentration of OH^-, [M]
R	Gas law constant, [J/(mol K)]
r_L	Reaction rate of solid lignin, [s^{-1}]
T	Temperature, [K]
T_B	Temperature of autoclave oil bath, [K]
t	Time, [s]
x_i	Mass fraction of dissolved lignin i = [1, 2, ..., 7], [-]
y	Position along the thickness of the wood chip, [m]
y, *norm*	Relative position along the thickness of the wood chip, [-]
z	Position along the thickness of the cell wall, [m]
z, *norm*	Relative position along the thickness of the cell wall, [-]
α	Ratio between mass of carbohydrates and lignin removed during pulping, [-]
β	Factor relating consumption of OH^- to the reaction of lignin and carbohydrates, [-]
δ	Radius of lumen, [μm]

https://doi.org/10.1021/acs.iecr.6c00374
Ind. Eng. Chem. Res. 2026, 65, 12938−12949

ε Wood chip porosity, [-]
λ Limiting ionic conductance in water at 298 K, $\left[\frac{A}{cm^2} \times \frac{V}{cm} \times \frac{g_{equiv}}{cm^2}\right]$
μ Dynamic viscosity, [kg/(m s)]
ρ_L Density of the lignocellulosic matrix, [kg/m^3]
τ Characteristic time of diffusion, [s]

Subscripts

B Conditions in the "lumen" boundary
C Conditions in the wood chip
i Index denoting dissolved lignin fractions
W Conditions in the cell wall

REFERENCES

(1) Johansson, M. T.; Broberg, S.; Ottosson, M. Energy Strategies in the Pulp and Paper Industry in Sweden: Interactions between Efficient Resource Utilisation and Increased Product Diversification. *J. Clean. Prod.* **2021**, *311*, No. 127681.
(2) Rahman, M.; Avelin, A.; Kyprianidis, K. A Review on the Modeling, Control and Diagnostics of Continuous Pulp Digesters. *Process. 2020* **2020**, *8* (10), 1231.
(3) Sjöström, E. *Wood Chemistry: Fundamentals and Applications*; Academic Press, San Diego, 1993.
(4) Gierer, J. Chemical Aspects of Kraft Pulping. *Wood Sci. Technol.* **1980**, *14* (4), 241−266.
(5) Nieminen, K.; Sixta, H. Comparative Evaluation of Different Kinetic Models for Batch Cooking: A Review. *Holzforschung* **2012**, *66* (7), 791−799.
(6) Inalbon, M. C.; Zanuttini, M. Dynamics of the Effective Capillary Cross-Sectional Area during the Alkaline Impregnation of Eucalyptus Wood. *Holzforschung* **2008**, *62* (4), 397−401.
(7) Ghaffari, R.; Almqvist, H.; Nilsson, R.; Lidén, G.; Larsson, A. Mass Transport of Lignin in Confined Pores. *Polymers (Basel)* **2022**, *14* (10), 1993.
(8) Bijok, N.; Fiskari, J.; Gustafson, R. R.; Alopaeus, V. Modelling the Kraft Pulping Process on a Fibre Scale by Considering the Intrinsic Heterogeneous Nature of the Lignocellulosic Feedstock. *Chem. Eng. J.* **2022**, *438*, No. 135548.
(9) Dang, V. Q.; Nguyen, K. L. A Universal Kinetic Model for Characterisation of the Effect of Chip Thickness on Kraft Pulping. *Bioresour. Technol.* **2008**, *99* (5), 1486−1490.
(10) Simão, J. P. F.; Carvalho, M. G. V. S.; Baptista, C. M. S. G. Heterogeneous Studies in Pulping of Wood: Modelling Mass Transfer of Dissolved Lignin. *Chem. Eng. J.* **2011**, *170* (1), 264−269.
(11) Brännvall, E.; Reimann, A. The Balance between Alkali Diffusion and Alkali Consuming Reactions during Impregnation of Softwood. Impregnation for Kraft Pulping Revisited. *Holzforschung* **2018**, *72* (3), 169−178.
(12) Kron, L.; Marion De Godoy, C.; Hasani, M.; Theliander, H. Kraft Cooking of Birch Wood Chips: Differences between the Dissolved Organic Material in Pore and Bulk Liquor. *Holzforschung* **2023**, *77* (8), 598−609.
(13) Grénman, H.; Wärnå, J.; Mikkola, J. P.; Sifontes, V.; Fardim, P.; Murzin, D. Y.; Salmi, T. Modeling the Influence of Wood Anisotropy and Internal Diffusion on Delignification Kinetics. *Ind. Eng. Chem. Res.* **2010**, *49* (20), 9703−9711.
(14) Gilbert, W.; Allison, B.; Radiotis, T.; Dort, A. A Simplified Kinetic Model for Modern Cooking of Aspen Chips. *Nord. Pulp Pap. Res. J.* **2021**, *36* (3), 399−413.
(15) Bijok, N.; Fiskari, J.; Gustafson, R. R.; Alopaeus, V. Chip Scale Modelling of the Kraft Pulping Process by Considering the Heterogeneous Nature of the Lignocellulosic Feedstock. *Chem. Eng. Res. Des.* **2023**, *193*, 13−27.
(16) Li, J.; Phoenix, A.; Macleod, J. M. Diffusion of Lignin Macromolecules Within the Fibre Walls of Kraft Pulp. Part I: Determination of the Diffusion Coefficient under Alkaline Conditions. *Can. J. Chem. Eng.* **1997**, *75* (1), 16−22.
(17) Brännvall, E.; Rönnols, J. Analysis of Entrapped and Free Liquor to Gain New Insights into Kraft Pulping. *Cellulose* **2021**, *28* (4), 2403−2418.
(18) Liu, Z.; Suntio, V.; Kuitunen, S.; Roininen, J.; Alopaeus, V. Modeling of Mass Transfer and Reactions in Anisotropic Biomass Particles with Reduced Computational Load. *Ind. Eng. Chem. Res.* **2014**, *53* (10), 4096−4103.
(19) Kron, L.; Hasani, M.; Theliander, H. Heterogenous Diffusion and Reaction Model of Kraft Delignification at the Cell Wall Level. *Ind. Eng. Chem. Res.* **2025**, *64* (3), 1497−1507.
(20) Luostarinen, K. Relationship of Selected Cell Characteristics and Colour of Silver Birch Wood after Two Different Drying Processes. *Wood Mater. Sci. Eng.* **2006**, *1* (1), 21−28.
(21) Marion de Godoy, C.; Laçaj, E.; Hackenstrass, K.; Galluccio, L.; Yu, H.; Florisson, S.; Wohlert, M.; Hall, S. A.; Hasani, M.; Theliander, H. Impregnation and delignification during kraft pulping of hardwood chips: characterization using *in-situ* X-ray tomography. *Wood Sci. Technol.* **2026**, *60*, 52.
(22) Svedman, M.; Tikka, P.; Luhtanen, M. Effects of Softwood Morphology and Chip Thickness on Pulping with a Displacement Kraft Batch Process. *Tappi Journal.* **1998**, *81* (7), 157−168.
(23) Stone, J. E. The Effective Capillary Cross-Sectional Area of Wood as a Function of PH. *Tappi J.* **1957**, *40* (7), 539−541.
(24) Smith, C. C. Studies of the Mathematical Modelling, Simulation, and Control of the Operation of a Kamyr Continuous Digester for the Kraft Process. Ph.D. Dissertation, Purdue University, 1974.
(25) Giudici, R.; Park, S. W. Kinetic Model for Kraft Pulping of Hardwood. *Ind. Eng. Chem. Res.* **1996**, *35* (3), 856−863.
(26) Suleiman, B. M.; Larfeldt, J.; Leckner, B.; Gustavsson, M. Thermal Conductivity and Diffusivity of Wood. *Wood Sci. Technol.* **1999**, *33* (6), 465−473.
(27) Poling, B. E.; Prausnitz, J. M.; O'Connell, J. P. *Properties of Gases and Liquids*, 5th ed.; McGraw-Hill Education, New York, 2001.
(28) McKibbins, S. Application of Diffusion Theory to the Washing of Kraft Cooked Wood Chips. *Tappi J.* **1960**, *43* (10), 801−805.
(29) Zhang, X. Z.; Ni, Y.; Van Heiningen, A. R. P. Effect of Consistency on Chemical Pulp Ozonation: Calculation of the Effective Capillary Cross-Sectional Area (ECCSA) and Tortuosity (λ) of the Fiber Wall. *Fifth European Workshop on LignoCellulosics and Pulp*; Aveiro, Portugal, 1998; pp 413−416.
(30) Marion de Godoy, C.; Hasani, M.; Theliander, H. Kraft Pulping of Model Wood Chips: Local Impact of Process Conditions on Hardwood Delignification and Xylan Retention. *Holzforschung* **2024**, *78* (8), 446−458.
(31) Marion de Godoy, C.; Andersson, M.; Hasani, M.; Theliander, H. Uniformity of Delignification during Kraft Pulping of Hardwood Chips: Impact of Wood Structure and the Importance of Impregnation. *Wood Sci. Technol.* **2026**, *60*, 49.
(32) Bogren, J.; Brelid, H.; Theliander, H. Reaction Kinetics of Softwood Kraft Delignification - General Considerations and Experimental Data. *Nord. Pulp Pap. Res. J.* **2007**, *22* (2), 177−183.
(33) Zanuttini, M.; Citroni, M.; Martínez, M. J.; Marzocchi, V. Chemimechanical Pulping of Poplar Wood. Alkaline Wood Pretreatment at Low Temperature. *Holzforschung* **1998**, *52* (4), 405−409.
(34) Santos, R. B.; Jameel, H.; Chang, H.-m.; Hart, P. W. Kinetics of Hardwood Carbohydrate Degradation during Kraft Pulp Cooking. *Ind. Eng. Chem. Res.* **2012**, *51* (38), 12192−12198.
(35) Nieminen, K.; Paananen, M.; Sixta, H. Kinetic Model for Carbohydrate Degradation and Dissolution during Kraft Pulping. *Ind. Eng. Chem. Res.* **2014**, *53* (28), 11292−11302.
(36) Santos, A.; Rodríguez, F.; Gilarranz, M. A.; Moreno, D.; García-Ochoa, F. Kinetic Modeling of Kraft Delignification of Eucalyptus Globulus. *Ind. Eng. Chem. Res.* **1997**, *36* (10), 4114−4125.
(37) Santiago, A. S.; Pascoal Neto, C.; Vilela, C. Impact of Effective Alkali and Sulfide Profiling on Eucalyptus Globulus Kraft Pulping. Selectivity of the Impregnation Phaseand Its Effect on Final Pulping Results. *J. Chem. Technol. Biotechnol.* **2008**, *83* (3), 242−251.

https://doi.org/10.1021/acs.iecr.6c00374
Ind. Eng. Chem. Res. 2026, 65, 12938−12949

(38) Mattsson, C.; Hasani, M.; Dang, B.; Mayzel, M.; Theliander, H. About Structural Changes of Lignin during Kraft Cooking and the Kinetics of Delignification. *Holzforschung* **2017**, *71* (7−8), 545−553.
(39) Manuscript in preparation. Kron, L.; Hasani, M.; Theliander, H. On the Mechanistic and Kinetic Role of Hydrogen Sulphide during Kraft Delignification. 2026.
(40) Gullichsen, J.; Kolehmainen, H.; Sundqvist, H. On the Non-Uniformity of the Kraft Cook. *Pap. ja Puu* **1993**, *74* (6), 486−490.

https://doi.org/10.1021/acs.iecr.6c00374
Ind. Eng. Chem. Res. 2026, 65, 12938−12949